

Dileptons from Disoriented Chiral Condensates

Yuval Kluger[†], Volker Koch, Jørgen Randrup, and Xin-Nian Wang

*Nuclear Science Division, Lawrence Berkeley National Laboratory,
University of California, Berkeley, CA 94720, USA*

Abstract

Disoriented chiral condensates or long wavelength pionic oscillations and their interaction with the thermal environment can be a significant source of dileptons. We calculate the yield of such dilepton production within the linear sigma model, both in a quantal mean-field treatment and in a semi-classical approximation. We then illustrate the basic features of the dilepton spectrum in a schematic model. We find that dilepton yield with invariant mass near and below $2m_\pi$ due to the soft pion modes can be up to two orders of magnitude larger than the corresponding equilibrium yield.

PACS: 11.30.Rd, 12.38.Mh, 25.75.-q

[†] Current address: Theoretical Division, Los Alamos National Laboratory, Los Alamos, NM 87545, USA.

1 Introduction

If the quark masses are neglected in two-flavor QCD, there would be a continuum of degenerate vacua in which chiral symmetry is spontaneously broken. These vacua are mutually related by $SU(2)$ rotations and can be characterized by non-vanishing scalar (sigma), $\langle\sigma\rangle = \langle\bar{q}q\rangle$, and pseudo-scalar (pion), $\langle\pi_i\rangle = \langle\bar{q}\gamma_5\tau_i q\rangle$, quark condensates.

In the “Baked Alaska” scenario proposed by Bjorken, Kowalski, and Taylor [1], a space-time region protected by a hot shell from the normal vacuum (where $\langle\pi_i\rangle = 0$, $\langle\sigma\rangle \neq 0$) can relax to a misaligned vacuum with a non-vanishing pion condensate, or disoriented chiral condensate (DCC). After the dispersion of the hot shell, the DCC will then decay into normal vacuum by coherent emission of soft pions. In relativistic heavy-ion collisions, if the system maintains quasi-equilibrium through the chiral phase transition, the quark masses, though small, will prevent the correlation length from growing indefinitely. However, recent numerical studies of the linear sigma model [2, 3, 4, 5, 6, 7, 8, 9] have shown that a rapid cooling-like quenching can drive the system far out of equilibrium and lead to significant amplification of the soft pionic modes. The resulting occupation numbers may then become large and lead to the emission of many pions in the same isospin state. In such an ideal scenario, the neutral pion fraction f exhibits an anomalous distribution, $P(f) = 1/2\sqrt{f}$, which has been suggested as an experimental signal [10, 11, 12]. However, if several separate domains are formed (*i.e.* if the size of the system is large in comparison with the correlation length), as may well occur in heavy-ion collisions, the signal is correspondingly degraded and the distribution approaches its normal form, an approximately normal distribution centered around $f=\frac{1}{3}$ [13, 14]. More advanced methods of analysis would then be needed, such as the use of wavelets [15] or cumulative moments [16].

In addition to the hadronic signals, the electro-magnetic DCC signatures have also been also addressed [17, 18]. Since the electro-magnetic current is given by the third component of the isovector current, the isospin oscillation of a coherent pion field may produce photons and dileptons which could provide information on the early dynamical evolution of the DCC. In Ref. [17], this emission from the oscillation of the coherent pion field was found to be sizable only for very small invariant masses, and thus it is hard to observe experimentally due to the large background from π_0 Dalitz decays. However, a DCC may also contribute to the incoherent production of dileptons. In particular, high-momentum incoherent pions may annihilate with the coherent DCC pions. Since the pion phase-space density in a DCC is comparatively large and well localized in momentum space, this process should lead to a considerable enhancement in the dilepton spectrum at finite invariant masses ($\simeq 2m_\pi$) that is rather narrow in invariant mass as well as transverse momentum.

Since the dynamical evolution leading to DCC formation is far from equilibrium, we shall study the electromagnetic production processes within the framework of time-dependent field theory, using both a quantal mean-field treatment [19] and a semi-classical approximation [20]. As these calculations treat coherent and incoherent production on an equal footing, the results do not depend on how that distinction is made. Therefore, to provide a simple understanding of the phenomenon, including the different contributions

from coherent and incoherent production, we shall subsequently illustrate the essential features by means of a schematic model.

This paper is then organized as follows. In the next section, we first briefly review the formulas needed to calculate the dilepton production. We then describe the dynamical calculations obtained with the linear sigma model and present the corresponding results for the dilepton yields. Finally, we turn to the schematic model.

2 Dilepton production from DCC

In general, in a non-equilibrium system, such as the dynamical evolution of DCC fields, the in and out states are not asymptotic states and the density matrices describing the system are not diagonal (except in isospin and charge). In this paper, we will neglect quantum effect caused by the off-diagonal matrices of the system in the calculation of the dilepton production. Therefore, the dilepton production yield can be given by the S matrices of the electromagnetic transition between different states [21],

$$\begin{aligned}\frac{dN_{\ell^+\ell^-}}{d^4q} &= \frac{\alpha^2}{6\pi^3} \frac{B}{q^4} (q^\mu q^\nu - q^2 g^{\mu\nu}) W_{\mu\nu}(q) , \\ W_{\mu\nu}(q) &= \frac{1}{\mathcal{Z}} \int d^4x d^4y e^{-iq \cdot (x-y)} \text{Tr}[\hat{\rho} \hat{j}_\mu(x) \hat{j}_\nu^\dagger(y)] ,\end{aligned}\quad (1)$$

where we have summed over the final states, $\mathcal{Z} = \text{Tr}[\hat{\rho}]$, and

$$B = (1 - \frac{4m_\ell^2}{q^2})^{1/2} (1 + \frac{2m_\ell^2}{q^2}) . \quad (2)$$

Since we are interested in the production of electron-positron pairs, we shall neglect the lepton mass m_ℓ in the following, i.e. $B = 1$.

We have modified the temporal integration boundaries from the asymptotic times $t = \pm\infty$ to finite initial and final times t_i and t_f . This is suitable for an initial-value problem where the initial conditions are fixed in non-asymptotic states which are assumed to be formed in a relativistic nuclear collision.

The Lagrangian density of the linear sigma model is given by

$$\mathcal{L} = \frac{1}{2} \partial_\mu \phi \partial^\mu \phi - \frac{1}{4} \lambda (\phi^2 - v^2)^2 + H \sigma , \quad (3)$$

where $\phi = (\sigma, \boldsymbol{\pi})$ are the chiral fields in $O(4)$ representation. The parameters, λ , v and H are determined by the pion and sigma mass, m_π , m_σ , and the pion decay constant f_π . In order to include electromagnetic (EM) processes, we can introduce an EM field in the charged sector of the above Lagrangian. The symmetrized EM current density coincides with the third component of the isovector current density and is given by

$$\hat{j}_\mu(x) = \frac{i}{2} [\hat{\pi}^\dagger(x) \overset{\leftrightarrow}{\partial}_\mu \hat{\pi}(x) - \hat{\pi}(x) \overset{\leftrightarrow}{\partial}_\mu \hat{\pi}^\dagger(x)] = \hat{\pi}_1(x) \partial_\mu \hat{\pi}_2(y) - \hat{\pi}_2(x) \partial_\mu \hat{\pi}_1(y) , \quad (4)$$

where the complex charged pion field operators are related to the Cartesian components by

$$\hat{\pi}(x) = \frac{1}{\sqrt{2}}[\hat{\pi}_1(x) + i\hat{\pi}_2(x)] , \quad \hat{\pi}^\dagger(x) = \frac{1}{\sqrt{2}}[\hat{\pi}_1(x) - i\hat{\pi}_2(x)] . \quad (5)$$

We shall neglect the quadratic coupling in the gauged linear sigma model and the anomalous electromagnetic coupling of π^0 , which all contribute to the dilepton production only to higher orders in the fine structure constant $\alpha = e^2/4\pi$.

2.1 Mean-field treatment

In the mean-field treatment, the four-point functions in the current-current correlator in Eq. (1) are given as products of two- and one-point functions similar to the decomposition of a free field four-point function according to Wick's theorem. Since the one-point functions then represent the average field they vanish for the pions. For uniform density matrices the contributions from two-point functions in the coincidence limit vanish since $\langle \hat{j}^\mu(x) \rangle = 0$. Furthermore correlators of the type $\langle \hat{\pi}(x)\hat{\pi}(y) \rangle$ or $\langle \hat{\pi}^\dagger(x)\hat{\pi}^\dagger(y) \rangle$ contribute only to zero-momentum processes and vanish altogether for the initial conditions chosen in the present calculations. Therefore, the only remaining components for the current-current correlator are of the type $\langle \hat{\pi}(x)\hat{\pi}^\dagger(y) \rangle$. The current-current correlator then takes the form,

$$\begin{aligned} W_{\mu\nu}(x, y) &= \langle \hat{\pi}^\dagger(x)\hat{\pi}(y) \rangle \langle \partial_\mu \hat{\pi}(x) \partial_\nu \hat{\pi}^\dagger(y) \rangle + \langle \partial_\mu \hat{\pi}^\dagger(x) \partial_\nu \hat{\pi}(y) \rangle \langle \hat{\pi}(x)\hat{\pi}^\dagger(y) \rangle \\ &- \langle \partial_\mu \hat{\pi}(x)\hat{\pi}^\dagger(y) \rangle \langle \hat{\pi}^\dagger(x)\partial_\nu \hat{\pi}(y) \rangle - \langle \partial_\mu \hat{\pi}^\dagger(x)\hat{\pi}(y) \rangle \langle \hat{\pi}(x)\partial_\nu \hat{\pi}^\dagger(y) \rangle. \end{aligned} \quad (6)$$

For a system in thermal equilibrium at the temperature T , the ensemble average is $\langle \cdot \rangle_{th} = \text{Tr}[\hat{\rho}_{th} \cdot]$, where $\hat{\rho}_{th} \sim e^{-\hat{H}/T}$. For free pions, the eigenstates are plane waves and the thermal ensemble average can be expressed accordingly,

$$\begin{aligned} \langle \hat{\pi}^\dagger(x)\hat{\pi}(y) \rangle_{th} &= \int \frac{d^3k}{2\omega_k(2\pi)^3} [n_k^+ e^{ik \cdot (x-y)} + (1 + n_k^-) e^{-ik \cdot (x-y)}] , \\ \langle \hat{\pi}(x)\hat{\pi}^\dagger(y) \rangle_{th} &= \int \frac{d^3k}{2\omega_k(2\pi)^3} [n_k^- e^{ik \cdot (x-y)} + (1 + n_k^+) e^{-ik \cdot (x-y)}] , \end{aligned} \quad (7)$$

where $n_k^\pm = 1/(e^{\omega/T} - 1)$ are the Bose-Einstein occupation numbers for the charged pions.

The hadronic tensor (6) entering into the dilepton-production expression then becomes

$$\begin{aligned} \frac{W_{\mu\nu}^{th}(q)}{d^4x} &= \int \frac{d^3k_1}{2\omega_1(2\pi)^3} \frac{d^3k_2}{2\omega_2(2\pi)^3} (2\pi)^4 \{ (k_1 - k_2)_\mu (k_1 - k_2)_\nu \\ &\cdot [n_{k_1}^- n_{k_2}^+ \delta^4(q - k_1 - k_2) + (1 + n_{k_1}^-)(1 + n_{k_2}^+) \delta^4(q + k_1 + k_2)] \\ &+ (k_1 + k_2)_\mu (k_1 + k_2)_\nu [n_{k_1}^- (1 + n_{k_2}^-) + n_{k_1}^+ (1 + n_{k_2}^+)] \delta^4(q - k_1 + k_2) \} , \end{aligned} \quad (8)$$

where we have taken advantage of the translational invariance in space and time to obtain the ensemble average *rate* of production by dividing by the corresponding four-volume $V(t_f - t_i)$.

The three terms in the above relation correspond to pion pair annihilation, creation and bremsstrahlung, respectively. The factor $1 + n_k^\pm$ is a result of the Bose enhancement in the final states. For dilepton production ($q^2 > 0$, $q_0 > 0$) only the pair annihilation term remains due to energy and momentum conservation. However, as we shall discuss briefly in section 3, once the pion dispersion relation develops several branches due to interactions, one can simply replace $n_k^\pm (1 + n_k^\pm)$ by $\sum_i n_k^\pm(i) [\sum_i (1 + n_k^\pm(i))]$ in the above equation with summation over the number of branches in the dispersion relation. Since dileptons can be emitted via the transition from one branch to another, all the terms, except the pair creation process, are allowed.

When the system is not in equilibrium, as is generally the case in a collision scenario, the current-current correlator cannot be expressed explicitly. However, in the present mean-field approximation the pion field vanishes on the average, and so the pion field operators can be expanded in terms of the annihilation and creation operators for medium-modified charged pions,

$$\hat{\pi}(x, t) \equiv \int \frac{d^3k}{(2\pi)^3} e^{i\mathbf{k}\cdot\mathbf{x}} [f_k(t) \hat{a}_k + f_k^*(t) \hat{b}_{-k}^\dagger] . \quad (9)$$

where the coefficients are the time-dependent mode functions $f_k(t)$.

The time evolution of the mode functions can be obtained in the mean-field approximation and we can then obtain the two-point correlation functions in Eq. (6), as described in Ref. [7, 19]. To solve the time evolution of the mode functions one needs to specify the initial conditions of the mean-field $\langle \sigma \rangle$ and its time derivative, the mode functions and their time derivatives, the average occupation numbers for each mode $\langle \hat{a}_k^\dagger \hat{a}_k \rangle \equiv n_k^+$, $\langle \hat{b}_k^\dagger \hat{b}_k \rangle \equiv n_k^-$ and their pair correlation $\langle \hat{a}_k \hat{b}_{-k} \rangle \equiv F_k$.

In order to have a finite set of renormalized equations, we have to choose the mode functions so that the high-momentum modes coincide with the zeroth order adiabatic vacuum described by

$$f_k(t_0) = \frac{1}{\sqrt{2\omega_k(t_0)}}, \quad \dot{f}_k(t_0) = \left[-i\omega_k(t_0) - \frac{\dot{\omega}_k(t_0)}{2\omega_k(t_0)} \right] f_k(t_0) , \quad (10)$$

with $\omega_k^2(t_0) = k^2 + \langle \chi(t_0) \rangle$ and $\chi = \lambda(\hat{\phi}^2/8 - v^2)$.

In this study, we will select ensembles with $n_k^+ = n_k^-$ and vanishing pair correlations, $F_k = 0$. By calculating two- and four-point functions the parameters λ , H , and v were chosen to give the best fit to the physical observables f_π , m_π , and the $\delta_s^{I=0}$ phase shifts [7]. In these simulations the bare coupling constant is $\lambda = 20$, the momentum cutoff is $\Lambda = 1$ GeV, the pion mass is 135 MeV and the pion decay constant is $f_\pi = 92.5$ MeV. The resulting mass of the σ is 340 MeV.

We investigate two different initial ensembles and evolve them from time $t_i = -50$ fm/c to $t_f = 50$ fm/c. All cases were prepared with equivalent energy densities and with zero kinetic energy density associated with the σ mean-field. The vacuum adiabatic mode functions are assumed as

$$f_k(t_0) = \frac{e^{-i\omega_k t_0}}{\sqrt{2\omega_k}} , \quad \dot{f}_k(t_0) = -i\omega_k f_k(t_0) . \quad (11)$$

The first one is an ensemble which at the initial time ($t = -50$ fm/c) has a mean σ field which is slightly perturbed around a thermal ensemble prepared at $T=100$ MeV. The initial quasiparticle frequency in this case is given by

$$\omega_k^2 = k^2 + \langle \chi \rangle, \quad (12)$$

with the initial value $\langle \chi \rangle = (138 \text{ MeV})^2$. The initial value of the mean σ field is 87 MeV. The average quasiparticle population n_k is given by the corresponding Bose-Einstein distribution and the energy density is then $\epsilon = 13.7 \text{ MeV/fm}^3$. At this relatively low temperature, the ensemble should be close to that of free pions and the results may thus serve to assess the quality of the calculation. Subsequently, we will call these initial conditions *thermal*.

The second ensemble is prepared with a negative value of χ in order to emulate a quench scenarios. In order to initialize the unstable pion modes (those having a negative value of ω_k^2), we have employed the relation $\omega_k^2 = k^2 + m_\pi^2 + (\langle \chi \rangle - m_\pi^2) \exp(-f_\pi^4/k^4)$, using the initial value $\langle \chi \rangle = -(132 \text{ MeV})^2$. [We note that at a large momentum the frequency agrees with the adiabatic vacuum frequency, as required by renormalization.] The initial value of the mean field is $\langle \sigma \rangle = 31 \text{ MeV}$ and the energy density is $\epsilon = 13.6 \text{ MeV/fm}^3$, *i.e.* similar to the equilibrium scenario. In the quench case, the initial quasiparticle modes are unoccupied, $n_k = 0$, corresponding to the local vacuum.

Let us now turn to the results for dilepton production. In Fig. 1 we show the dilepton yield obtained by using the mode functions generated from the thermal initial conditions to calculate the current-current correlation function in Eq. (6) (full lines). Note that we have divided the yield by the total space-time volume, $V\Delta t$, it is therefore the averaged production rate during the time interval $\Delta t = t_f - t_i$. We show the results for two different values of the three momentum of the dilepton, $q = 50 \text{ MeV}$ and $q = 200 \text{ MeV}$. This is compared with the analytical result for a free-pion gas (dashed lines),

$$\frac{1}{VT} \frac{dN_{\ell^+\ell^-}^{(2)}}{dM d^3q} = \frac{\alpha^2}{48\pi^4} \frac{q_0}{M} \left(1 - \frac{4m_\pi^2}{M^2}\right) \int_{\omega^-}^{\omega^+} \frac{d\omega}{q} n_k^+ n_{q-k}^-, \quad (13)$$

with $\omega^\pm = (q_0 \pm q\sqrt{1 - 4m_\pi^2/M^2})/2$ and $q_0 = \sqrt{M^2 + q^2}$. As compared to the analytical result for the free pion gas, the numerical calculation based on the thermal mode functions give a contribution below the two-pion threshold as well. This contribution is spurious as it arises from the finite resolution of the energy δ function in our calculation: Since the Fourier transform in time extents only over a finite time interval, the energy is not perfectly conserved. As a result the terms proportional to $n_{k_1}(1 + n_{k_2})$ in Eq. (8) do contribute to the time-like sector while with perfect energy conservation their contribution is restricted to space-like photons only. This spill-over from the space-like region is amplified because of the factor $1/q^4$ in Eq. (1). In addition to leading order this contribution depends on linearly on the distribution function n_k and is thus further enhanced by $1/n_k \gg 1$ with respect to the pion annihilation term.

In order to verify this, we have also performed a calculation with the mode functions of a free pion gas. The result is indistinguishable from the one obtained with the dynamical mode functions, showing that the interaction plays a negligible role at $T=100$ MeV.

By inspecting the individual contributions, we have also verified that the spurious contribution is indeed due to the terms proportional to $n_{k_1}(1 + n_{k_2})$. At the present stage, this spurious contribution forms an numerical background. It is also responsible for the slight disagreement between the analytical and numerical results for the free pions above the two-pion threshold. With this numerical background in mind, let us turn now to the

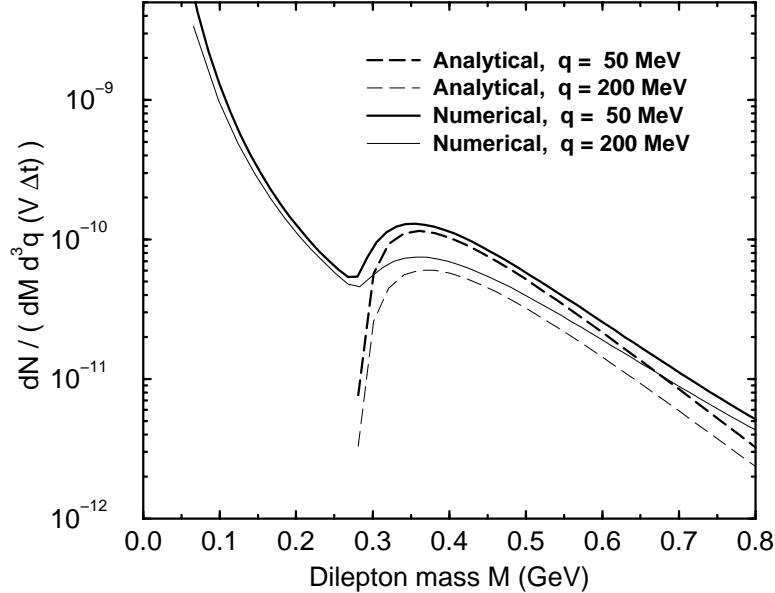


Figure 1: Dilepton invariant mass spectrum for the thermal initial conditions for two values of the three momentum q (full lines). Also shown are the theoretical results for a free pion gas (dashed lines).

comparison between the thermal and quench initial conditions, as illustrated in Fig. 2. Clearly, around an invariant mass of $M \simeq 2m_\pi$ the dilepton production rate from the quench initial conditions is about two orders of magnitude larger than the thermal production. This enhancement is less for larger momenta, reflecting the narrow momentum distribution of pions in the DCC fields. Furthermore, at low invariant masses there seems to be an enhancement as predicted in Ref. [17]. Because of our numerical background, we are not able to give a quantitative estimate of this enhancement. However, due to the strong background from the π_0 Dalitz decay, this enhancement is difficult to measure experimentally. Therefore, let us concentrate on the enhancement around $M \simeq 2m_\pi$. As expected from the narrow momentum distribution of the DCC pions, this enhancement is localized in invariant mass as well as in transverse momentum. The latter can be seen from Fig. 3 where the dilepton yield is plotted as a function of the three-momentum of the dilepton for an invariant mass of $M = 300$ MeV. The enhancement is confined to low momenta, below $q \simeq 300$ MeV. While the localization of the enhancement in invariant

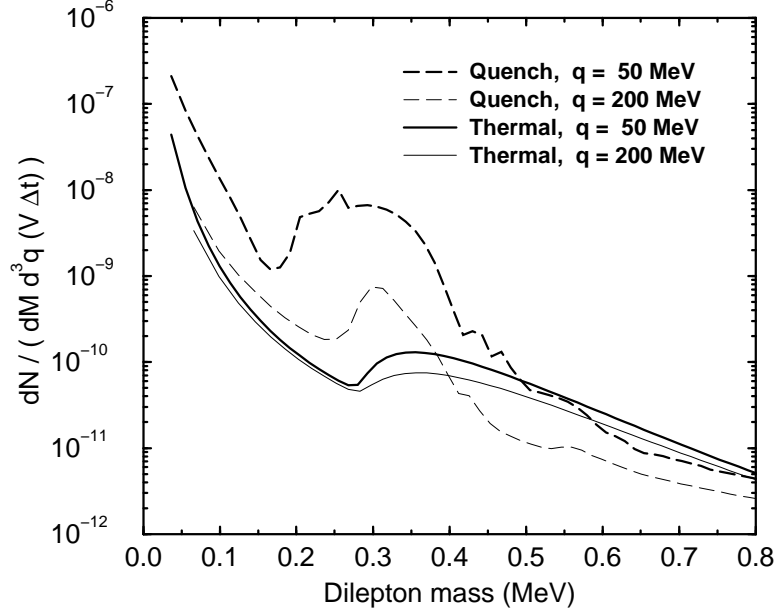


Figure 2: Dilepton invariant mass spectra for thermal (full lines) and quench (dashed lines) initial conditions. Shown are the spectra for two different values of the three dilepton three momentum q .

mass nicely reflects the enhancement of low-momentum pion modes, it may be very difficult to observe experimentally. At low transverse momentum the background from false pairs is largest and it remains to be seen if present detector designs allow a sufficiently accurate subtraction to make the extraction of this signal feasible. In order to get an idea about the experimental constraints, we have subjected our results to the CERES acceptance cuts [22]. The resulting invariant mass spectrum is virtually indistinguishable from the thermal one. Only if the momentum cuts can be pushed down to $\simeq 100$ MeV will an enhancement of about a factor of ten remain.

2.2 Semi-classical treatment

In order to verify that our results are robust with respect to model details, we have also calculated dilepton production with a different treatment of the linear sigma model, namely the semi-classical approach described in Ref. [20]. In that treatment, the system is described by the real field $\phi(\mathbf{r}, t) = (\sigma, \boldsymbol{\pi})$, which is evolved by the classical equation of motion,

$$[\square + \lambda(\phi^2 - v^2)]\phi = H\hat{\sigma} , \quad (14)$$

where $\phi^2 = \phi \circ \phi$ and $\hat{\sigma}$ denotes a unit vector along the σ axis. In the present context, when we are concerned with dilepton production in a macroscopically uniform system,

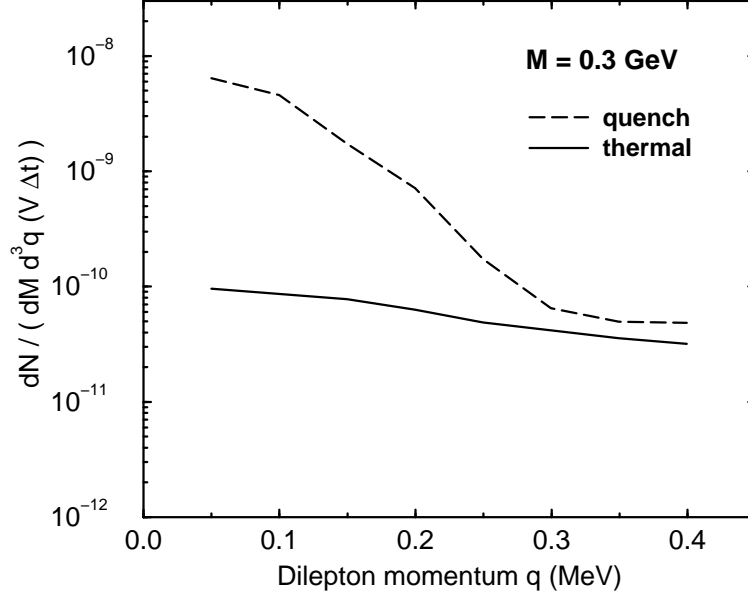


Figure 3: Momentum spectra for thermal (full lines) and quench (dashed lines) initial conditions for dilepton pairs of invariant mass $M = 300$ MeV.

it is natural to enclose the system in a (sufficiently large) box with periodic boundary conditions. The spatial average of the field can then be considered as the order parameter, $\underline{\phi}(t) = \langle \phi(\mathbf{r}, t) \rangle$, and the residual fluctuations represent quasi-particle excitations relative to that constant field, $\delta\phi(\mathbf{r}, t) = \phi(\mathbf{r}, t) - \underline{\phi}(t)$. A similar separation holds for the time derivative of the field.

In order to solve the above equation of motion, it is necessary to specify the initial field configuration, $\phi(\mathbf{r}, t_i)$, and the associated time derivative. Employing the method developed in Ref. [20], we sample these initial conditions from a thermal ensemble at a specified temperature T . The occupation numbers $n_{\mathbf{k}}$ of the quasi-particle modes are drawn from the appropriate Bose-Einstein distributions which ensures that the initial state displays the proper quantum-statistical features. The resulting treatment is then akin to the Vlasov model often employed in nuclear dynamics at moderate energies, which is the semi-classical analogue of the Time-Dependent Hartree-Fock description.

In order to make contact with the quantum mean-field studies described earlier, we consider two scenarios having the same energy, namely thermal equilibrium at $T=140$ MeV and a corresponding quenched initial condition. The quenched ensemble has been generated from the thermal ensemble by suppressing the field fluctuations by a factor of 100 and resetting the order parameter to $\underline{\phi}(t_i) = (\sigma_0, \mathbf{0})$, with a vanishing time derivative, $\underline{\psi}(\mathbf{r}, t_i) = (0, \mathbf{0})$. Using $\sigma_0 = 32$ MeV ensures that the energy of the quenched scenario matches the thermal value, which is about 40 MeV/fm^3 .

The numerical solution of the equations of motion of the chiral fields yields the evolu-

tion of the Cartesian components of the pion field, $\boldsymbol{\pi}(\mathbf{r}, t)$, in addition to the sigma field $\sigma(\mathbf{r}, t)$. The corresponding electromagnetic current density is then easy to extract,

$$J_\mu(x) = \pi_1(x) \partial_\mu \pi_2(x) - \pi_2(x) \partial_\mu \pi_1(x) . \quad (15)$$

In order to calculate the associated invariant differential dilepton yield, we employ the following expression [21],

$$\frac{d^4 N}{d^4 q} = \frac{2}{3\pi} \left(\frac{\alpha}{2\pi} \right)^2 \left(\frac{q^\mu q^\nu}{q^4} - \frac{g^{\mu\nu}}{q^2} \right) \int d^4 x \int d^4 y J_\mu(x) e^{-iq(x-y)} J_\nu(y) \quad (16)$$

$$= \frac{2}{3\pi} \left(\frac{\alpha}{2\pi} \right)^2 \tilde{J}_\mu^*(q) \left(\frac{q^\mu q^\nu}{q^4} - \frac{g^{\mu\nu}}{q^2} \right) \tilde{J}_\nu(q) . \quad (17)$$

This expression ignores the final-state Bose enhancement factors $1+n_{\mathbf{k}}$ which is justified when the occupation number $n_{\mathbf{k}}$ is small, as is typically the case in equilibrium [20]. In particular, for $T=140$ MeV the occupancy of the lowest quasi-particle mode is about 0.30. However, the occupancy may reach several units in the corresponding quench scenario and the formula (16) may then significantly underestimate the contribution from the softest pion modes¹.

The last expression (17) recasts the dilepton yield in terms of the four-dimensional Fourier transform of the charge current,

$$\tilde{J}_\mu(q) = \int d^4 x J_\mu(x) e^{iqx} = \int_{t_i}^{t_f} dt \int_V d\mathbf{r} J_\mu(\mathbf{r}, t) e^{iq_0 t - i\mathbf{q} \cdot \mathbf{r}} . \quad (18)$$

The factorized form (17) is of great numerical convenience, since the transform $\tilde{J}_\mu(q)$ can be readily accumulated in the course of each dynamical history, and the contraction in (17) need only be carried out at the end of the evolution. In (16) and (18) the time integration extends over the duration of the observation, from t_i to t_f . In the equilibrium scenario, the yield then becomes proportional to $\Delta t = t_f - t_i$ as well as to the volume V , and so a division by the four-volume $V\Delta t$ yields the corresponding invariant production rate $d^4 N / (d^4 q (V\Delta t))$.

In general, we consider an entire sample of \mathcal{N} individual evolutions, $\{\phi^{(n)}(\mathbf{r}, t)\}$, where the label n enumerates the individual “events” in the sample. The resulting ensemble-average dilepton yield is then

$$\langle \frac{d^4 N}{d^4 q} \rangle = \frac{1}{\mathcal{N}} \sum_{n=1}^{\mathcal{N}} \frac{d^4 N^{(n)}}{d^4 q} , \quad (19)$$

where $d^4 N^{(n)} / d^4 q$ is the contribution from the particular event n , obtained as described above. Since we consider ensembles that have translational symmetry, the current-current

¹ It may be noted that if the calculated pion field $\boldsymbol{\pi}(\mathbf{r}, t)$ is assumed to represent a standard coherent state, then the quantal evaluation of the dilepton radiation rate would lead to the above expression (16) when the commutator terms are ignored; if those commutator terms were retained, then the final-state Bose enhancement factors would be recovered.

correlation function, $\prec J_\mu(x) J_\nu(y) \succ$, will depend only on the spatial separation. Moreover, in the special case of an equilibrium ensemble, its temporal dependence in equilibrium is only via the time difference. [In practice, the considered dilepton observables vary little from event to event, because the system is larger than the correlation length, and therefore sufficiently accurate results can be obtained on the basis of rather small samples.]

In order to verify that the adopted method indeed leads to physically reasonable results, let us consider the production of back-to-back dileptons from a thermal gas of free pions. In that special case, the four-momentum of the dilepton is of the form $q = (M, \mathbf{0})$ and we are interested in masses M above $2m_\pi$. The current-current contraction in (16) is then especially simple and it is elementary to show that its ensemble average is given by

$$\prec J_\mu(x) \left(\frac{q^\mu q^\nu}{q^2} - g^{\mu\nu} \right) J_\nu(y) \succ = \prec \mathbf{J}(x) \cdot \mathbf{J}(y) \succ = 2|\nabla C|^2 - 2C\Delta C, \quad (20)$$

where we have employed the thermal correlation function of the charged pion fields,

$$\prec \pi_1(x)\pi_1(y) \succ = \prec \pi_2(x)\pi_2(y) \succ = C(\mathbf{r}, t) = \frac{1}{V} \sum_{\mathbf{k}} \frac{\tilde{n}_k}{\omega_k} \cos(\mathbf{k} \cdot \mathbf{r} - \omega_k t), \quad (21)$$

with \tilde{n}_k being the thermal occupancy, $\tilde{n}_k = 1/(\exp(\omega_k/T) - 1)$, and (\mathbf{r}, t) denoting the difference $x-y$. [The adopted sampling procedure ensures that the numerically extracted correlation function indeed yields this expression [20].] Since the back-to-back dileptons have vanishing momentum, $\mathbf{q} = \mathbf{0}$, the Fourier transform over the separation \mathbf{r} reduces to a spatial average and we readily find

$$\int_V d\mathbf{r} \prec \mathbf{J}(x) \cdot \mathbf{J}(y) \succ = 4 \int_V d\mathbf{r} |\nabla C(\mathbf{r}, t)|^2 = \frac{2}{V} \sum_{\mathbf{k}} \frac{\tilde{n}_k^2}{\omega_k^2} k^2 [1 + \cos 2\omega_k t]. \quad (22)$$

The remaining Fourier transformation over the temporal difference then restricts the contributions in the sum to those modes that have frequencies ω_k near half the dilepton mass, $M/2$. Thus, in the continuum limit, when both the box and the time interval are large, we recover exactly the usual expression for production of dileptons by pion annihilation,

$$\frac{d^4 N^{th}}{d^4 q d^4 x} = \frac{4}{3\pi} \left(\frac{\alpha}{2\pi} \right)^2 \int \frac{d\mathbf{k}}{(2\pi)^3} \int dt \frac{\tilde{n}_k^2}{\omega_k^2} \frac{k^2}{M^2} [1 + \cos 2\omega_k t] e^{iMt} = \frac{\alpha^2}{3} \frac{n_0^2}{(2\pi)^4} \left(1 - \frac{4m_\pi^2}{M^2} \right)^{\frac{3}{2}}, \quad (23)$$

where n_0 denotes the occupancy of pion states with the matching frequency $\omega_0 = M/2$. Thus, at the formal level, the semi-classical method is indeed physically reasonable.

In order to illustrate the numerical reliability of the calculations, we consider again the simple case of a free pion gas in thermal equilibrium, in analogy with what was shown in Fig. 1. Figure 4 shows both the analytical result for the invariant dilepton production rate and the corresponding results obtained by integrating the equation of motion for the free fields, with the initial field configurations having been sampled from the associated thermal

ensemble as described above. As in the case of the mean-field treatment, the numerical calculation yields a reasonable result for dilepton masses above the pion annihilation threshold, but exhibit a divergent behavior for lower masses as a reflection of the pole at $q = 0$. The fluctuations in the numerical results are a consequence of the much coarser grid employed in the semi-classical calculations: the system is confined within a cubic torus of size $L=24$ fm (with a grid spacing of 0.24 fm) and 41 modes have been included in each of the three Cartesian directions, for a total of 68,921 modes. Moreover, the time evolution has been performed only up to 50 fm/c.

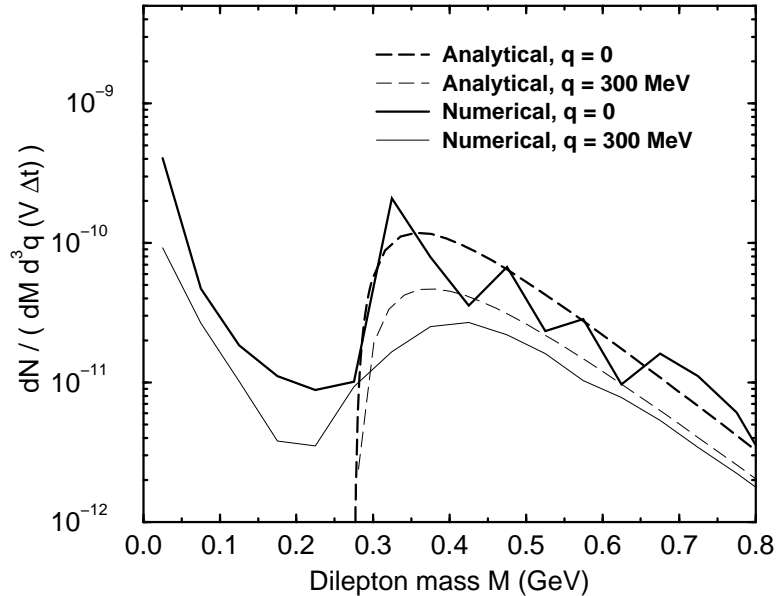


Figure 4: The invariant dilepton production rate in a gas of free pions in thermal equilibrium at $T = 100$ MeV. The solid curves are obtained by solving the free-field equations numerically, while the dashed curves represent the corresponding analytical results. The heavy curves are for back-to-back production, $q = 0$, while the light curves are for a finite momentum of the dilepton, $q = 300$ MeV.

We now move on to discuss the results of the numerical simulations in the two scenarios described above. Figure 5 shows the invariant production rate as a function of the dilepton mass $M = \sqrt{q^2}$, for various magnitudes of its momentum \mathbf{q} , in a display similar to Fig. 1. The results are qualitatively similar to those obtained with the mean-field treatment: the quench scenario leads to a large enhancement around 400 MeV. In the present case the enhancement is only about one order of magnitude, because the coarser grid considered leads to a quicker damping of the oscillations in the order parameter and, consequently, the amplification of the soft pions modes is less extreme. Still, there is clearly a very significant effect of the non-equilibrium evolution.

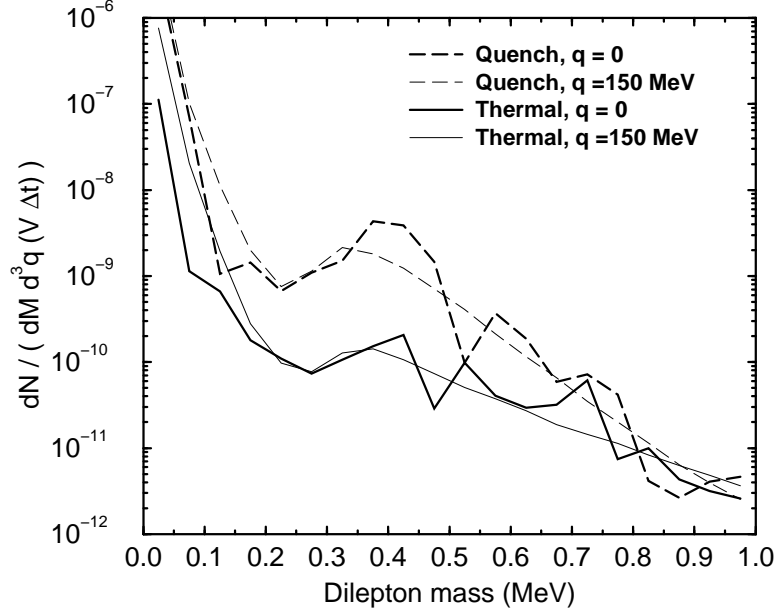


Figure 5: The invariant mass spectrum for both thermal initial conditions (solid curves) and the corresponding quench scenario (dashed curves), for either back-to-back dileptons having $\mathbf{q}=\mathbf{0}$ (heavy curves) and dileptons with a finite momentum of $q=150$ MeV (light curves).

Finally, Fig. 6 shows the effective production rate $d^4N/(dM d^3q (V \Delta t))$ as a function of the magnitude of the dilepton momentum \mathbf{q} , for dilepton masses near $M=300$ MeV. Again, we see how the non-equilibrium evolution following the quench caused a large enhancement of the slow-moving dileptons. The results of the two calculations agree qualitatively: The quench initial conditions lead to a substantial enhancement of the dilepton yield at invariant masses close to $M \simeq 2m_\pi$. The calculation based on the quantal mean-field approximation (section 2.1) predicts a considerably stronger enhancement which is also more narrow in invariant mass as well as momentum. As we will explain in the following section this implies that in the quantal mean-field approximation the enhancement of the low momentum modes is stronger and narrower in momentum space than in the semi-classical approximation. Translated into the DCC language, the DCC fields generated in the quantal mean-field approximation have a larger field strength and are of larger spatial extent. There are several possible reasons for this quantitative difference. First, the Bose enhancement factors, present in the mean-field treatment, certainly will increase the dilepton yield to some extent. Second, the comparatively coarse grid employed in the semi-classical treatment leads to a faster dampening of the oscillations in the order parameter, resulting in a smaller amplification of the soft pion modes. Finally, the semi-classical treatment incorporates the mode mixing arising from the non-linear form of the interaction. This mechanism helps to equilibrate the system and thus redistribute

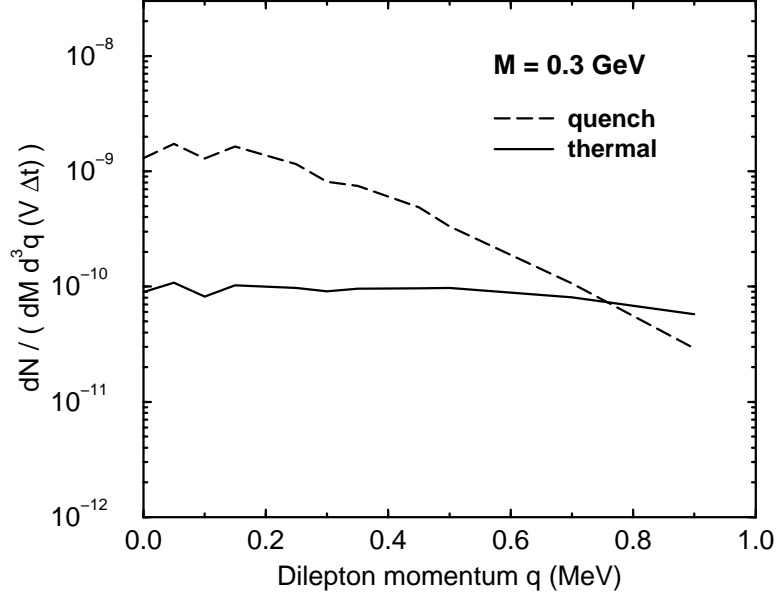


Figure 6: The production rate ($d^4N/dM d^3q (V \Delta t)$) as a function of the magnitude of the dilepton momentum \mathbf{q} , for dilepton masses near $M=300$ MeV.

the strength gained by the low-momentum modes. While it would be interesting to see if the inclusion of mode mixing in the quantal mean-field formulation reduces the enhancement, it will be hard to give a precise quantitative estimate of their effect. Therefore, it is probably more reasonable to consider the quantitative difference between the two approximations as an inherent uncertainty which can only be resolved by experiment. We note, however, that the above difference clearly demonstrates that a precise measurement of the dilepton spectrum not only can reveal the presence of DCC configurations but can also provide information about their size as well as their strength.

3 A schematic model

With the mean-field and semi-classical treatments, the time-dependent fields are dynamically coupled to the quasi-particle modes and the soft and hard modes of the fields are treated on an equal footing. To understand the main features of dilepton production due to the soft modes, we shall now consider the dilepton production process in a schematic model in which the soft and hard modes are coupled only via the electromagnetic interaction causing dilepton production. The hard modes are then represented by a thermal gas of pions having a specified temperature T , while the soft modes will be evolved dynamically according to the one-dimensional Bjorken expansion scenario. Hence the density operator can be factorized, $\hat{\rho} = \hat{\rho}_{th} \otimes \hat{\rho}_{DCC}$, where $\hat{\rho}_{th}$ is the normalized density opera-

tor for the thermal gas and $\hat{\rho}_{DCC}$ is the normalized density operator for the soft modes, referred to as the DCC field.

The current-current correlator $\hat{W}_{\mu\nu}(q)$ can then be decomposed according to how many thermal pions are involved in the dilepton production process. The first term represents the coherent emission of dileptons from DCC fields alone and involves no thermal pions,

$$W_{\mu\nu}^{(0)}(q) = \int d^4x d^4y \langle \hat{j}_\mu(x) \hat{j}_\nu^\dagger(y) \rangle_{DCC} e^{-iq \cdot (x-y)} = \langle \hat{j}_\mu(q) \hat{j}_\nu^\dagger(q) \rangle_{DCC} . \quad (24)$$

where the DCC expectation value is $\langle \cdots \rangle_{DCC} = \text{Tr}[\hat{\rho}_{DCC} \cdots]$.

Contributions to the current-current correlator from processes involving a thermal pion are

$$\begin{aligned} W_{\mu\nu}^{(1)}(x, y) &= \langle \hat{\pi}^\dagger(x) \hat{\pi}(y) \rangle_{DCC} \langle \partial_\mu \hat{\pi}(x) \partial_\nu \hat{\pi}^\dagger(y) \rangle_{th} - \langle \partial_\mu \hat{\pi}^\dagger(x) \partial_\nu \hat{\pi}(y) \rangle_{DCC} \langle \hat{\pi}(x) \hat{\pi}^\dagger(y) \rangle_{th} \\ &+ \langle \partial_\mu \hat{\pi}^\dagger(x) \hat{\pi}(y) \rangle_{DCC} \langle \hat{\pi}(x) \partial_\nu \hat{\pi}^\dagger(y) \rangle_{th} - \langle \partial_\mu \hat{\pi}(x) \hat{\pi}^\dagger(y) \rangle_{DCC} \langle \hat{\pi}^\dagger(x) \partial_\nu \hat{\pi}(y) \rangle_{th} \\ &+ \text{c.c.} , \end{aligned} \quad (25)$$

where we have omitted the vanishing disconnected part and all other terms containing $\langle \hat{\pi}^\dagger(x) \hat{\pi}^\dagger(y) \rangle_{th}$ or $\langle \hat{\pi}(x) \hat{\pi}(y) \rangle_{th}$ which vanish in a thermal equilibrium environment. Using Eq. (7), we obtain

$$\begin{aligned} W_{\mu\nu}^{(1)}(q) &= \int \frac{d^3k}{2\omega_k (2\pi)^3} \left\{ (2k_\mu + q_\mu)(2k_\nu + q_\nu) [(1 + n_k^+) \langle \hat{\pi}^\dagger(-q - k) \hat{\pi}(-q - k) \rangle_{DCC} \right. \\ &+ (1 + n_k^-) \langle \hat{\pi}(q + k) \hat{\pi}^\dagger(q + k) \rangle_{DCC}] + (2k_\mu - q_\mu)(2k_\nu - q_\nu) \\ &\cdot [n_k^+ \langle \hat{\pi}(q - k) \hat{\pi}^\dagger(q - k) \rangle_{DCC} + n_k^- \langle \hat{\pi}^\dagger(k - q) \hat{\pi}(k - q) \rangle_{DCC}] \Big\} , \end{aligned} \quad (26)$$

The first two terms in the above equation correspond to the emission of one pion together with a dilepton by the DCC field. The factor $1 + n_k^\pm$ is a result of the Bose enhancement in the final state. The second two terms proportional to n_k^\pm represent the annihilation or absorption of one thermal pion by the DCC field.

From Eq. (26) one can readily see how the momentum distribution of the DCC field is imprinted onto the dilepton spectrum. Once the momentum of the dilepton is large compared to the inverse of the DCC domain size, the integral no longer has support from the Fourier transform of the pion field $\langle \hat{\pi}^\dagger(k \pm q) \hat{\pi}(k \pm q) \rangle_{DCC}$, which restricts the contribution to low momenta and to a small window in invariant mass. For example, if one considers a classical field that oscillates with a typical frequency of $\omega \simeq m_\pi$ and has a Gaussian distribution of width R_\perp in coordinate space, one can see from Eq. (26) that the dilepton yield will be concentrated around an invariant mass of $M \simeq 2m_\pi$. The width of this distribution will be of the order of $1/R_\perp$ in invariant mass as well as in the three-momentum \mathbf{q} .

Within this schematic model, it is possible to take approximate account of expansion by subjecting the DCC field to a boost-invariant Bjorken expansion. The DCC field depends then only on the proper time $\tau = \sqrt{t^2 - z^2}$ and, in the linear sigma model, its equation of motion becomes

$$\ddot{\phi} + \frac{1}{\tau} \dot{\phi} + \lambda(\phi^2 - v^2)\phi = H\hat{\sigma} . \quad (27)$$

The initial values of ϕ and $\dot{\phi}$ are sampled from normal distributions with suitable width parameters. The corresponding energy-momentum tensor is then relatively simple,

$$T^{\mu\nu} = \epsilon_K(2u^\mu u^\nu - g^{\mu\nu}) + \epsilon_V g^{\mu\nu}, \quad (28)$$

where the four-velocity is $u^\mu = \tilde{x}^\mu/\tau$ with $\tilde{x}_\mu \equiv (t, 0, 0, z)$. The contribution to the energy density from the time dependence of the field is $\epsilon_K = \frac{1}{2}\dot{\phi}^2$, while the contribution from the interaction is $\epsilon_V = \frac{\lambda}{4}(\phi^2 - v^2)^2 - H\sigma - \epsilon_{\text{gs}}$, with the vacuum energy being $\epsilon_{\text{gs}} = \frac{\lambda}{4}(f_\pi^2 - v^2)^2 - Hf_\pi$. The expansion causes the energy density to drop steadily,

$$\frac{\partial}{\partial\tau}(\epsilon_K + \epsilon_V) = -2\frac{\epsilon_K}{\tau}, \quad (29)$$

and a simple power behavior is quickly approached, $\epsilon_K + \epsilon_V \rightsquigarrow \epsilon_0\tau_0/\tau$. The coefficient ϵ_0 then provides a convenient means of characterizing the particular solution. The limiting $1/\tau$ behavior of the energy density is a general characteristic of the boost invariant scenario [9] and we therefore assume that the energy density of the thermal gas drops in the same manner. This is accomplished by using a time-dependent temperature for the gas, $T = (\tau_0/\tau)^{1/4}T_0$.

We can take approximate account of the finite transverse size of a DCC domain by giving the chiral fields a common profile (such that the orientation of the pion field in the Cartesian space only depends on the proper time),

$$g(x_\perp) = \exp(-x_\perp^2/2R_\perp^2). \quad (30)$$

This transverse profile is simply an ansatz and does not follow from nor is subjected to the equation of motion. Such a simple Gaussian form was suggested by numerical simulations [5] and it suffices for our present purpose. The electromagnetic current density then becomes [17]

$$j_\mu(x) = v_3 f_\pi^2 \frac{\tilde{x}_\mu}{\tau^2} g^2(x_\perp) = v_3 f_\pi^2 \frac{\tilde{x}_\mu}{\tau^2} \exp(-x_\perp^2/R_\perp^2). \quad (31)$$

where the dimensionless normalization coefficient v_3 is determined by the specific initial condition.

The longitudinal expansion causes the current density to decrease as the proper time grows. As a consequence, the contribution to the dilepton yield from the coherent dilepton emission remains finite. Following Ref. [17], and averaging over the ensemble of initial conditions, we find

$$\frac{dN_{\ell^+\ell^-}^{(0)}}{dy_q dq_\perp^2 dM} = \frac{\alpha^2}{24} \pi^2 R_\perp^4 e^{-q_\perp^2 R_\perp^2/4} f_\pi^4 \prec v_3^2 \succ \frac{q_\perp^2}{M^3 M_\perp^2} [J_0^2(M_\perp \tau_0) + N_0^2(M_\perp \tau_0)], \quad (32)$$

where the transverse mass is $M_\perp = \sqrt{M^2 + q_\perp^2}$ (with $M^2 = q^2$) and J_0 and N_0 are Bessel functions. This differential yield is independent of the dilepton rapidity because of the boost invariance of the DCC field, and so it depends only on the initial value of the current, as determined by the ensemble average $\prec v_3^2 \succ$. It may also be noted that the coherent

emission vanishes as the transverse momentum of the dilepton photon approaches zero. This further diminishes the importance of coherent emission compared to the incoherent emission at low transverse momenta where the effect of the DCC is expected to be largest.

In order to calculate the incoherent dilepton production by the DCC field, we need to perform the Fourier transformation of pion field $\boldsymbol{\pi}(x) = \boldsymbol{\pi}(\tau)g(x_\perp)$. We find

$$\pi_i(\pm p) = \begin{cases} \pi G(p_\perp) \int_{\tau_0}^{\infty} \tau d\tau \pi_i(\tau) [-N_0(M_\perp \tau) \mp i J_0(M_\perp \tau)] , & p_0 \geq |p_\parallel| \\ 2G(p_\perp) \int_{\tau_0}^{\infty} \tau d\tau \pi_i(\tau) K_0(M_\perp \tau) , & |p_0| \leq |p_\parallel| \end{cases} \quad (33)$$

where $M_\perp = \sqrt{|p_0^2 - p_\parallel^2|}$ and $G(q_\perp) = \pi R_\perp^2 \exp(-q_\perp^2 R_\perp^2/4)$.

One can then use $\langle \pi^\dagger(q)\pi(q) \rangle = \frac{1}{2}[\langle |\pi_1(q)|^2 \rangle + \langle |\pi_2(q)|^2 \rangle]$ in Eq. (26) to calculate the dilepton yield from the interaction of the thermal pions with the DCC field,

$$\begin{aligned} \frac{dN_{\ell^+\ell^-}^{(1)}}{dy_q dq_\perp^2 dM} &= \frac{2\alpha^2}{3\pi^2} \frac{1}{M} \int \frac{d^3k}{2\omega_k (2\pi)^3} \left[\frac{(k \cdot q)^2}{M^2} - m_\pi^2 \right] \\ &\quad \left[(1 + n_k^+) \langle \pi^\dagger(-q-k)\pi(-q-k) \rangle_{DCC} \right. \\ &\quad + (1 + n_k^-) \langle \pi(q+k)\pi^\dagger(q+k) \rangle_{DCC} \\ &\quad \left. + n_k^+ \langle \pi(q-k)\pi^\dagger(q-k) \rangle_{DCC} + n_k^- \langle \pi^\dagger(k-q)\pi(k-q) \rangle_{DCC} \right]. \end{aligned} \quad (34)$$

Due to the boost invariance, we need only consider dileptons with zero rapidity so that $q = (M_\perp, \mathbf{q}_\perp, 0)$. Given the simple Gaussian transverse profile of the pion field, one can carry out the azimuthal integral, and the remaining two-dimensional integral can then be evaluated numerically by use of the Fourier transforms in Eq. (33).

In the numerical evaluation of the dilepton production from the DCC field, we have employed the following rather conventional parameter values, $\lambda = 19.97$, $v = 87.4$ MeV, $f_\pi = 92.5$ MeV, $m_\pi = 135$ MeV, with which $H = f_\pi m_\pi^2 = (119 \text{ MeV})^3$ and $m_\sigma = \sqrt{2\lambda f_\pi^2 + m_\pi^2} = 600$ MeV. We first calculate the Fourier transformation of the pion fields according to Eq. (33) for the solution of the equation of motion. We then calculate $\langle \pi^\dagger(q)\pi(q) \rangle$ averaging over the initial configurations which then is used for the numerical evaluation of the dilepton yield in Eq. (34). The ensemble average $\langle v_3^2 \rangle$ is also extracted and used in the calculation of the coherent emission yield, Eq. (32).

Figure 7 shows the differential dilepton yield from a total space-time volume $\frac{1}{2}\pi R_\perp^2 (\tau_{\text{max}}^2 - \tau_0^2)$ due to incoherent emission from the DCC field together with the corresponding average thermal rate. We have used the following parameter values, $T_0 = 145$ MeV, $R_\perp = 2$ fm, $\tau_0 = 1$ fm, $\tau_{\text{max}} = 102.4$ fm, and the characteristic energy density carried by the DCC field was $\epsilon_0 = 58$ MeV/fm³, which is the same as the thermal pion energy density at the employed temperature T_0 . We have also separated the incoherent dilepton rate into bremsstrahlung and annihilation (absorption) part, since they are caused by very different processes and should have different features in the invariant mass spectrum.

We find that the coherent emission rate in Eq. (32) is negligible as compared to the incoherent emission. This is related to the fact that the coherent emission in our scenario depends only on the third component of the conserved isovector current. Because the

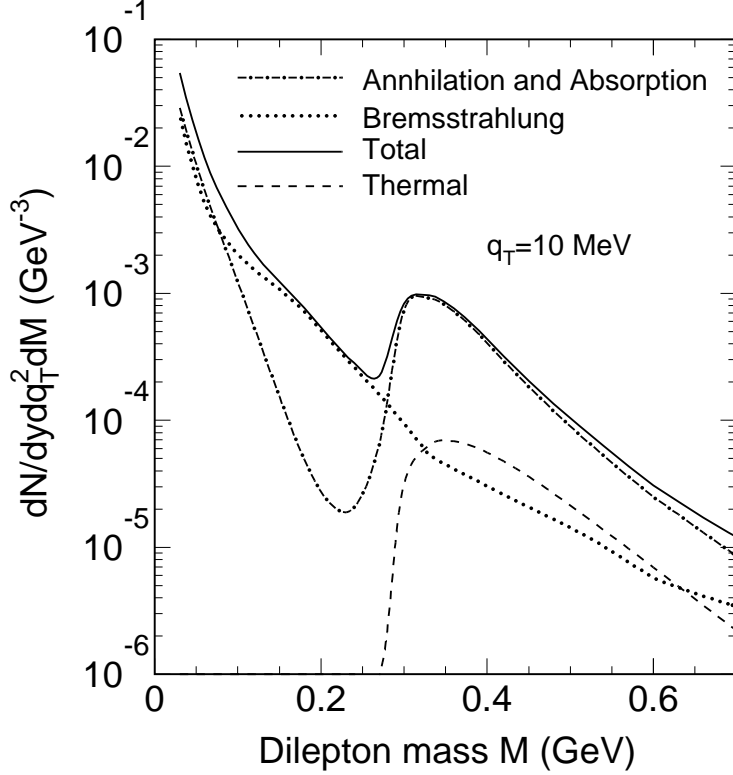


Figure 7: Dilepton spectrum from the DCC field, both bremsstrahlung (dotted), annihilation and absorption (dot-dashed), and their sum (solid), as well as the thermal emission (dashed). The initial temperature of the thermal environment is $T_0=145$ MeV, while the characteristic energy density carried by the DCC field is $\epsilon_0=58$ MeV/fm³.

energy density carried by the isovector current decreases much faster than that carried by other degrees of freedom, the associated dilepton emission is thus also less important. However, the incoherent dilepton emission is very significant in comparison with the thermal production. The spectrum from the pion annihilation and absorption by the DCC field (dot-dashed) has a structure manifest of two components in the second two terms in Eq. (34), depending on the energy flow. In the contribution from the annihilation with the DCC field, energy flows out of the DCC field, therefore the dilepton spectrum has a threshold at $M = 2m_\pi$, if the DCC pion field oscillate with a minimum frequency of m_π . If the energy flows into the DCC field, dileptons are then emitted when thermal pions are absorbed by the DCC field. The dilepton spectrum from these absorption processes has no threshold and dominates the annihilation and absorption spectrum at small invariant masses $M < m_\pi$, as seen in Fig. 7.

Shown as the dotted line in Fig. 7 is the dilepton spectrum due to pion bremsstrahlung from the DCC field, the first two terms in Eq. (34). Since the emitted pions have at least a minimum energy of m_π , the DCC field must have some higher frequencies in order to

emit a thermal pion plus a pair of leptons. This means that the DCC must have some quasi-particle modes whose masses are larger than the pion mass m_π . To illustrate this, we show in Fig. 8 both the pion and sigma fields as functions of time and their corresponding Fourier spectra. As one can clearly see, besides the normal pion mode with mass m_π (this is the frequency of the fields for the zero-momentum mode we are considering), there are others resonances with higher masses. While the resonances at $\simeq 3.5m_\pi$ and $\simeq 5.5m_\pi$ are clearly visible, the higher ones cannot be seen here due to their small amplitudes and the limited resolution due to the finite time interval used in our numerical calculation. These quasi-particle modes are normally referred to as parametric resonances in a non-linear and strongly coupled system. We will not elaborate on the interesting physics associated with the parametric resonances, but just point out that they play an important role in the preheating of the early universe [23] and the amplification of the long-wavelength pion mode following an extremely nonequilibrium initial condition [18, 24]. With these parametric resonances in mind, we can readily understand the spectrum of the dilepton from the bremsstrahlung processes: dileptons are produced via the transitions of the high resonances to the normal pion mode. As we increase the invariant mass of the dilepton, some of the transitions are gradually turned off as the energy of the dilepton becomes larger than the mass differences between the higher resonances and the normal pion mass m_π . This is why there is a slight oscillation in the bremsstrahlung dilepton spectrum. The oscillation vanishes when the invariant mass reaches the highest parametric resonance that the numerical solution can resolve. This is also the case when we increase the transverse momentum of the dilepton.

In Fig. 7 is also shown the sum of the different contributions to dilepton spectrum from the DCC field (solid curve) as well as the contribution from annihilation in the cooling pion gas. In general, one can see that the incoherent dilepton production below and near $2m_\pi$ threshold region is significantly larger than the thermal production. As we already pointed out, because of the finite spatial size of DCC field in the transverse direction, dileptons from the DCC field exhibit a much faster decrease with the transverse momentum q_\perp than those due to thermal production.

4 Summary

We have calculated the production of dileptons from disoriented chiral condensates using a quantal mean-field as well as a semi-classical treatment for the time evolution in the linear sigma model. We have compared the dilepton spectra obtained when using so called quench initial conditions, which lead to a strong enhancement of long wave length pion modes (DCC), with those obtained from thermal initial conditions. Compared to the thermal spectrum the quench initial conditions lead to a strong enhancement (factor 20 - 100 depending on the model) at an invariant mass of about $M \simeq 2m_\pi$. This enhancement is confined to dilepton momenta of $q \leq 300 - 500$ MeV and also rather narrow in invariant mass. Based on the analysis in a schematic model we find that the observed enhancement at $M \simeq 2m_\pi$ is due to the annihilation of thermal pions with those from the DCC.

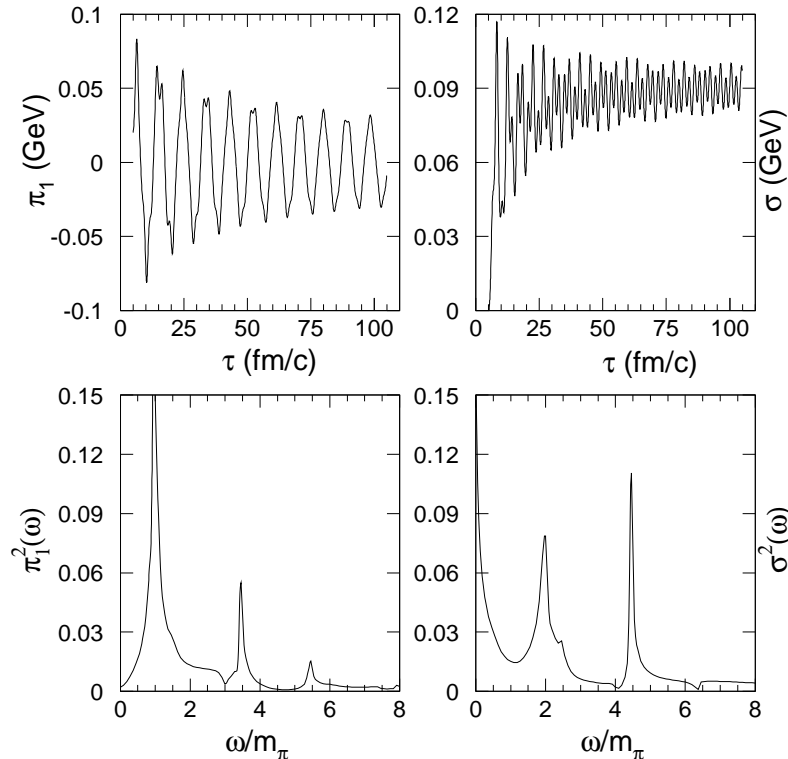


Figure 8: The time evolution of the π_1 and σ DCC field and their corresponding Fourier spectra.

We furthermore found some evidence for an enhancement at low invariant masses, $M < m_\pi$, which, however, we could not unambiguously establish due to numerical backgrounds. In the schematic model this enhancement is due to bremsstrahlung-type processes involving the absorption or emission of pions by and from the DCC. The latter reflects the rich dynamical structure of the DCC field. The spectral distribution of the pion field shows distinct peaks not only close to the pion mass but also at higher frequencies. This phenomenon is related to the so-called parametric resonances and is responsible for a comparatively strong dilepton yield as a result of pion emission processes.

Within the schematic model, we could also address the more realistic scenario of a longitudinal expansion. We find that the above enhancement remains also in this case.

Both dynamical solutions, which are based on distinct approximations to the linear sigma model, predict qualitatively the same enhancement: A large bump at $M \simeq 2m_\pi$ as well as an enhancement at low invariant masses. Overall, the quantal mean-field model seems to yield a larger enhancement than the semi-classical treatment. This quantitative difference may be due to several factors. First, the Bose enhancement factors are absent in the semi-classical treatment. Second, the semi-classical treatment incorporates the mode mixing resulting from the non-linear interaction and this mechanism tends to reduce the

number of pions in the DCC state. Both of these features lead to a somewhat smaller signal.

As far as experimental observation of this enhancement is concerned, it will be probably very difficult to see the enhancement at low invariant masses, $M < m_\pi$, because this region will be dominated by the Dalitz decay of the π^0 . The enhancement around $M \simeq 2m_\pi$ on the other hand should be observable in principle. In this mass range the major competing channel is the Dalitz decay of the η . From the analysis of CERN SPS data (see e.g. [25]) the η Dalitz is at most a factor of five stronger than the pion-annihilation channel. Therefore an enhancement of the pion annihilation by a factor of ten or larger should be visible. However, due to the background from false pairs it is very difficult to measure dileptons of small momentum [26] where the expected enhancement is located.

In the present work we have ignored expansion, with the exception of the schematic model. This will have to be taken into account in future work for a more realistic description of a heavy-ion collision. Moreover, expansion provides one possible justification of the quench initial conditions [9]. Certainly in a given effective theory, a consistent treatment should generate the quench conditions dynamically starting from a more or less thermal state at temperatures above T_c . The resulting dilepton spectrum from such a calculation should then provide a more realistic picture of possible enhancements to be expected in heavy ion experiments. In addition such a calculation needs to account for additional dissipative processes which are not included in the linear sigma model, such as the scattering with vector mesons.

However, too little is known about the physics that reigns close to the chiral phase transition to allow us to give a final theoretical answer about the existence of DCC states in relativistic heavy ion collisions. Therefore, experiments measuring unique observables, such as the one addressed here, will be needed to determine that issue and its implication for the chiral phase transition in matter.

Acknowledgments

We would like to thank J.D. Bjorken, J.-P. Blaizot, D. Boyanovsky, F. Cooper, A. Kovner, E. Mottola, and Z. Huang for stimulating discussions. This work was supported by the Director, Office of Energy Research, Office of High Energy and Nuclear Physics, Divisions of High Energy Physics and Nuclear Physics of the U.S. Department of Energy under Contract No. DE-AC03-76SF00098.

References

- [1] J.D. Bjorken, K.L. Kowalski, and C.C. Taylor, SLAC preprint SLAC-PUB-6109, Proc. of Les Rencontres de la Vallée D' Aoste, La Thuile, 1993, ed. M. Greco, Editions Frontier, p. 507 (1993).
- [2] K. Rajagopal and F. Wilczek, Nucl. Phys. **B404**, 577 (1993).

- [3] S. Gavin, A. Goksch, and R.D. Pisarski, Phys. Rev. Lett. **72** 2143, (1994).
- [4] S. Gavin and B. Müller, Phys. Lett. **B329**, 486 (1994).
- [5] M. Asakawa, Z. Huang, and X.-N. Wang Phys. Rev. Lett. **74**, 3126 (1995).
- [6] D. Boyanovsky, H.J. de Vega, and R. Holman, Phys. Rev. D **51**, 734 (1995).
- [7] F. Cooper, Y. Kluger, and E. Mottola, and J.P. Paz, Phys. Rev. **D51**, 2377 (1995).
- [8] Y. Kluger, F. Cooper, E. Mottola, Phys. Rev. **C54**, 3298 (1996).
- [9] J. Randrup, Phys. Rev. Lett. **77**, 1226 (1996).
- [10] A.A. Anselm and M.G. Ryskin, Phys. Lett. **B266**, 482 (1991).
- [11] J.-P. Blaizot and A. Krzywcki, Phys. Rev. **D46**, 246 (1992).
- [12] J.D. Bjorken, Acta Phys. Pol. **B23**, 561 (1992).
- [13] R.D. Amado and Y. Lu, Phys. Rev. **D54**, 7075 (1996).
- [14] J. Randrup, Nucl. Phys. **A616**, 531 (1997).
- [15] Z. Huang, I. Sarcevic, R. Thews, and X.-N. Wang, Phys. Rev. **D54**, 750 (1996).
- [16] T.C. Brooks, *et al.*, MiniMax Collaboration, hep-ph/9609375, 1996.
- [17] Z. Huang and X.-N. Wang, Phys. Lett. **B383**, 457 (1996).
- [18] D. Boyanovsky, H.J. de Vega, R. Holman, and J.F.J. Salgado, hep-ph/9608205, Phys. Rev. D in print.
- [19] Y. Kluger, J. M. Eisenberg, B. Svetitsky, F. Cooper, and E. Mottola, Phys. Rev. **D45**, 4659 (1992).
- [20] J. Randrup, Phys. Rev. **D55**, 1188 (1997).
- [21] L.D. McLerran and T. Toimela, Phys. Rev. **D31**, 545 (1985).
- [22] G. Agakichiev et al., Phys. Rev. Lett. **75**, 1272 (1995).
- [23] L. Kofman, A. Linde, and A.A. Starobinsky, Phys. Rev. Lett. **73**, 3195 (1994)
- [24] S. Mrowczynski and B. Müller, Phys. Lett. **B363**, 1 (1995).
- [25] V. Koch and C. Song, Phys. Rev. **C54** 1903 (1996).
- [26] J. Carroll, private communication, (1997).